Born−Oppenheimer ab Initio QM/MM Dynamics Simulations of Na^+ and K^+ in Water: From Structure Making to Structure Breaking Effects

Anan Tongraar, Klaus R. Liedl, and Bernd M. Rode*

Department of Theoretical Chemistry, Institute for General, Inorganic and Theoretical Chemistry, University of Innsbruck, Innrain 52a, A-6020 Innsbruck, Austria

Received: May 18, 1998

The description of nonadditive contributions in the first hydration shell of Na^+ and K^+ has been improved by performing molecular dynamics simulations based on combined ab initio quantum mechanical and molecular mechanical potentials. The active-site region, the first hydration sphere of ions, is treated by Born−Oppenheimer ab initio quantum mechanics, while the environment is described by classical pair potentials. The average coordination numbers obtained by this high accuracy method, with valence double-ζ basis sets for water and Los Alamos ECP plus DZ basis sets for cations, lead to a lower value of 5.6 ± 0.3 for Na^+ and a higher value of 8.3 ± 0.3 for K^+, respectively, compared to the corresponding values of 6.5 ± 0.2 and 7.8 ± 0.2 resulting from pair potentials. The effects of nonadditive terms are also found to play a significant role in the preferential orientation of water molecules within the first hydration shell of Na^+ and K^+. The experimentally observed "structure-breaking" effects of K^+ are well reflected and explained on a molecular basis by the simulation results.

1. Introduction

In the study of aqueous electrolyte solutions, alkali ion solutions are an interesting subject due to their important role in solution chemistry, biochemistry and pharmacology.[1,2] In particular, the contrasting behavior of Na^+ and K^+ in aqueous solution is of substantial interest especially concerning ionic pumps across the cell membrane.[3] Structural information about hydrated alkali ions has been obtained from both computer simulations and experiments.[4−17] Although experimental techniques, such as X-ray or neutron diffraction, are available to study the microscopic structure, the results are often prone to large errors for very dilute solution systems due to technical limitations.[18,19] Results from computer simulations can provide a more detailed interpretation and prediction of experimental observations at the molecular level. In the past decade, most studies have been carried out with simulation techniques based on assumed pairwise additivity in describing the interactions of particles[4,20−25] because of technical difficulties in constructing higher-order potential functions. It has also been found that the nonadditive contributions converge rather slowly and that the terms usually have alternating signs.[26] However, several studies have reported that the nonadditive contributions always play a more or less significant role and are sometimes even crucial to describing the properties of systems.[27−34] The neglect of these terms may artificially favor wrong geometrical arrangements and too high coordination numbers in the first solvation shell of ions.[27,35−37]

For the study of monovalent ions in water, such as Li^+, Na^+, and K^+, the effects of nonadditivity in the first solvation shell of these ions can be expected to be smaller than those for multiple charged ions. Nevertheless, the inclusion of three-body interaction terms in the intermolecular interaction potentials has been shown to improve the results, concerning the reproduction of experimental observations.[27,30,31] The use of potential functions including many-body terms, in the simplest case three-body terms,[38−40] is a useful way of improvement, but it is not an elegant way, and for higher terms it is increasingly complicated since their construction becomes very demanding and hardly tractable for large systems. Recently, a combined quantum mechanical (QM) and molecular mechanical (MM) procedure[41−43] has been introduced. This technique offers a breakthrough for correcting multiple many-body interactions in condensed-phase systems.[35−37] As nonadditive contributions in ionic aqueous solutions are substantial mostly in the first solvation shell only, the system can be partitioned into two parts, a quantum mechanical and a molecular mechanical region. The QM region, i.e., the first hydration sphere of the ion, is treated by Born−Oppenheimer ab initio quantum mechanics, while the rest of the system is described by molecular mechanics potential functions based on ab initio energy surfaces. Previous studies employing this method have pointed out that higher nonadditive terms can also play a significant role; that is, inclusion of three-body corrections alone is not adequate to describe structural properties correctly. For example, in the system of Li^+ in NH_3, the inclusion of three-body terms reduces the coordination number of Li^+ from 6 to 4.4,[44] whereas it is reduced further to 4[35] by the combined QM/MM simulation. By this high-accuracy technique, a tetrahedral structure has been recently found also for the hydration shell structure of Li^+, in contrast to the octahedral structure predicted by traditional simulations using pair potentials.[37] As a consequence, it was highly interesting to evaluate these effects for the hydration shell structures of Na^+ and K^+ as well by means of the combined QM/MM method.

2. Details of Calculations

2.1. Evaluation of Many-Body Interactions. To estimate the influence of many-body terms, energy optimizations of $M(H_2O)_n^+$, M = Na and K and $n = 1-4$, 6, and 8, were carried out using the DZV+P basis set for H_2O[45] and the Los Alamos

* Corresponding author.

10.1021/jp982270y CCC: $15.00
Published on Web 11/21/1998

TABLE 1: Optimized Geometries and Corresponding Many-Body Effects in $Na(H_2O)_n^+$ and $K(H_2O)_n^+$ Complexes

$M(H_2O)_n^+$	n	r_{M-O}[a]	r_{O-H}	$\angle_{HOH}$	ΔE_{ab}[b]	ΔE_{pair}	ΔE_{diff}	$\%E^{nbd}$
M = Na	1	2.27	0.95	106.0	−26.5	−26.5		
	2	2.29	0.95	106.0	−50.9	−52.3	1.4	2.7
	3	2.31	0.95	106.2	−70.8	−77.0	6.2	8.1
	4	2.37	0.94	105.9	−83.8	−92.7	8.8	9.5
	6	2.42	0.94	107.1	−109.7	−136.9	27.2	19.8
	8	2.51	0.94	108.2	−164.5	−246.1	81.6	33.2
M = K	1	2.68	0.95	105.5	−18.6	−18.6		
	2	2.71	0.95	105.6	−36.0	−37.1	1.1	2.9
	3	2.73	0.95	105.8	−50.6	−55.0	4.4	7.9
	4	2.77	0.95	105.8	−62.6	−68.1	5.5	8.1
	6	2.82	0.94	106.5	−84.5	−102.0	17.5	17.2
	8	2.89	0.94	107.6	−126.3	−185.8	59.5	31.9

[a] Experimental r_{M-O} values in the gas phase of M^+-H_2O are 2.26 and 2.60 Å for M = Na and K, respectively.[47] [b] Experimental enthalpies in the gas phase of M^+-H_2O are −24.0 and −17.9 kcal·mol^{-1} for M = Na and K, respectively.[47]

ECP plus DZ basis set for Na^+ and K^+.[46] Since many-body interactions are defined as the difference of the total interaction energy and the energy calculated from the sum of all pair interactions, the interaction energy differences, ΔE_{diff} can be calculated as

$$\Delta E_{diff} = \Delta E_{ab} - \Delta E_{pair} \quad (1)$$

where ΔE_{ab} denotes the total interaction energy of $M(H_2O)_n^+$ complexes, which can be computed using the supermolecular approach by

$$\Delta E_{ab} = E(M(H_2O)_n^+) - E(M^+) - nE(H_2O) \quad (2)$$

and ΔE_{pair} represents the sum of all pair interactions, which can be obtained by

$$\Delta E_{pair} = \sum_i^n [E(M^+ - H_2O^i) - E(M^+) - E(H_2O)] + \sum_{j>i}^n [E(H_2O^i - H_2O^j) - 2E(H_2O)] \quad (3)$$

Thus, the relative interaction energy differences, $\%E^{nbd}$, with respect to the pair potential can be calculated by

$$\%E^{nbd} = 100\left(1 - \frac{\Delta E_{ab}}{\Delta E_{pair}}\right) \quad (4)$$

The results of geometry optimizations and the corresponding data for the many-body effects are given in Table 1.

2.2. Molecular Dynamics Simulations. A flexible model, which includes intermolecular[48] and intramolecular interactions,[49] was employed for water. The pair potential functions for Na^+-H_2O and K^+-H_2O were newly constructed. The 1800 Hartree−Fock interaction energy points obtained from Gaussian 94[50] calculations using the DZV+P basis set for H_2O[45] and the Los Alamos ECP plus DZ basis set for Na^+ and K^+ [46] were fitted to the analytical forms

$$\Delta E_{Na^+-H_2O} = \sum_{i=1}^{3}\left(\frac{A_{ic}}{r_{ic}^4} + \frac{B_{ic}}{r_{ic}^8} + C_{ic}\exp(-D_{ic}r_{ic}) + \frac{q_i q_c}{r_{ic}}\right) \quad (5)$$

$$\Delta E_{K^+-H_2O} = \sum_{i=1}^{3}\left(\frac{A_{ic}}{r_{ic}^4} + \frac{B_{ic}}{r_{ic}^6} + C_{ic}\exp(-D_{ic}r_{ic}) + \frac{q_i q_c}{r_{ic}}\right) \quad (6)$$

TABLE 2: Optimized Parameters of the Analytical Pair Potential for the Interaction of Water with Na^+ and K^+ (Interaction Energies in kcal·mol^{-1} and Distances in angstroms)[a]

pair	A (kcal mol^{-1} Å^4)	B (kcal mol^{-1} Å^8)	C (kcal mol^{-1})	D (Å^{-1})
Na−O	−706.762 51	1392.0333	25 305.645	3.225 589 7
Na−H	33.622 581	173.849 01	19.141 491	0.871 375 8
pair	A (kcal mol^{-1} Å^4)	B (kcal mol^{-1} Å^6)	C (kcal mol^{-1})	D (Å^{-1})
K−O	−2364.1024	10 375.969	357.786 56	1.330 416 9
K−H	8.078 899 9	449.985 77	12.678 787	0.497 891 1

[a] The charges on Na, K, O, and H are 1.0, 1.0, −0.6598, and 0.3299, respectively.

where A, B, C, and D are the fitting parameters (see Table 2), r_{ic} denotes the distances between the cation and the i-th atom of water, and q are the atomic net charges. These two analytical functions have similar forms, except the use of different inverse powers in the B terms representing the best fit with smallest standard deviation. The global minima for the stabilization energies of these functions are −26.3 and −18.5 kcal·mol^{-1} for Na^+-H_2O and K^+-H_2O, respectively, with the corresponding cation−oxygen distances being 2.3 and 2.7 Å, in the direction of the dipole moment of water. These stabilization energies are in good agreement with the enthalpies of the reaction $M^+ + H_2O \rightarrow M^+-H_2O$ of −24.0 and −17.9 kcal·mol^{-1} reported by Kebarle et al.[47] (The error of the experiment was assumed to be in the range of ±1 to ±3 kcal·mol^{-1}.[51])

Classical molecular dynamics simulations using pair potentials were performed first. Afterward, the combined QM/MM molecular dynamics simulations were performed at the Hartree−Fock level using the DZV basis set for water and the Los Alamos ECP plus DZ basis set for cations (LANL2DZ basis set in Gaussian 94), starting from the equilibrium configurations obtained from the pair potential simulations. The reaction-field procedure[52] was employed for treatment of long-range interactions. The diameters of the first solvation shells of Na^+ and K^+ obtained in the pair potential simulations, namely 3.2 and 3.8 Å, were selected as the size of the QM region beyond which a smoothing function[53] starts. After an interval of 0.2 Å (i.e., up to 3.4 and 4.0 Å for the cases of Na^+ and K^+, respectively), this function leads smoothly into the MM region. By this method, n-body terms up to $n = 7-9$ are implicitly included in the simulation of the first hydration shell. All simulations were carried out in a canonical ensemble at 298 K with a time step of 0.2 fs. Assuming the density of pure water, a box length of 18.9 Å results for one cation in 199 water molecules. The classical molecular dynamics simulations started from random configurations and were equilibrated for 20 000 time steps. The simulations were continued for 60 000 time steps to collect configurations every tenth step. The combined QM/MM molecular dynamics simulations started with the reequilibration for 10 000 time steps, followed by another 10 000 time steps to collect configurations every fifth step. The quantum mechanical calculations and the simulations were performed on a SGI Power Challenge XL at the computing center, University of Innsbruck.

2.3. Selection of Basis Sets in QM/MM Simulations. The selection of basis set is a crucial choice, as the QM portion is the most expensive computational part in the QM/MM simulation (more than 95% of total CPU time). The LANL2DZ basis sets were selected since ab initio geometry optimizations using these basis sets reproduce structural properties rather well with

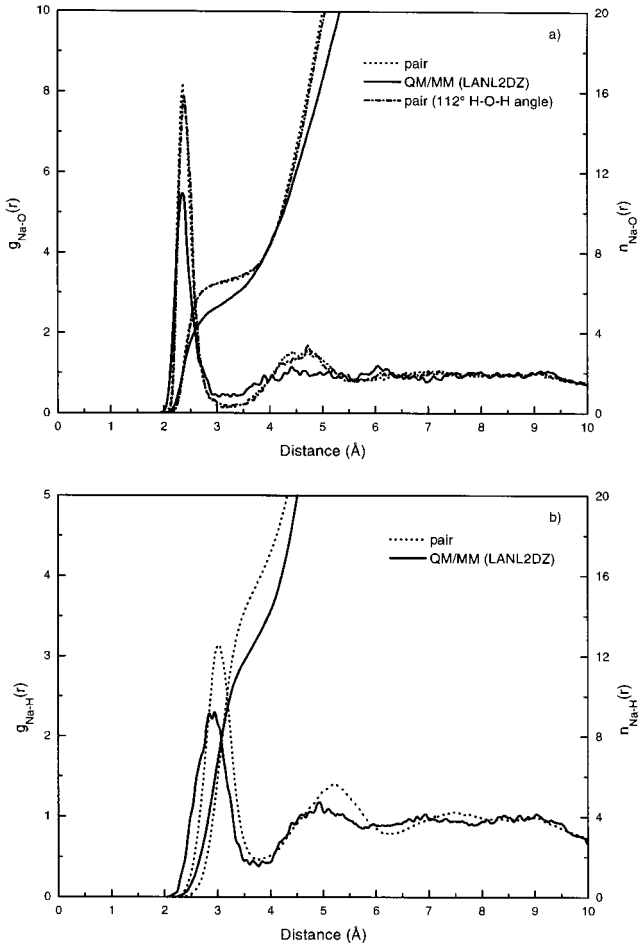

Figure 1. (a) Na−O and (b) Na−H radial distribution functions and their corresponding integration numbers.

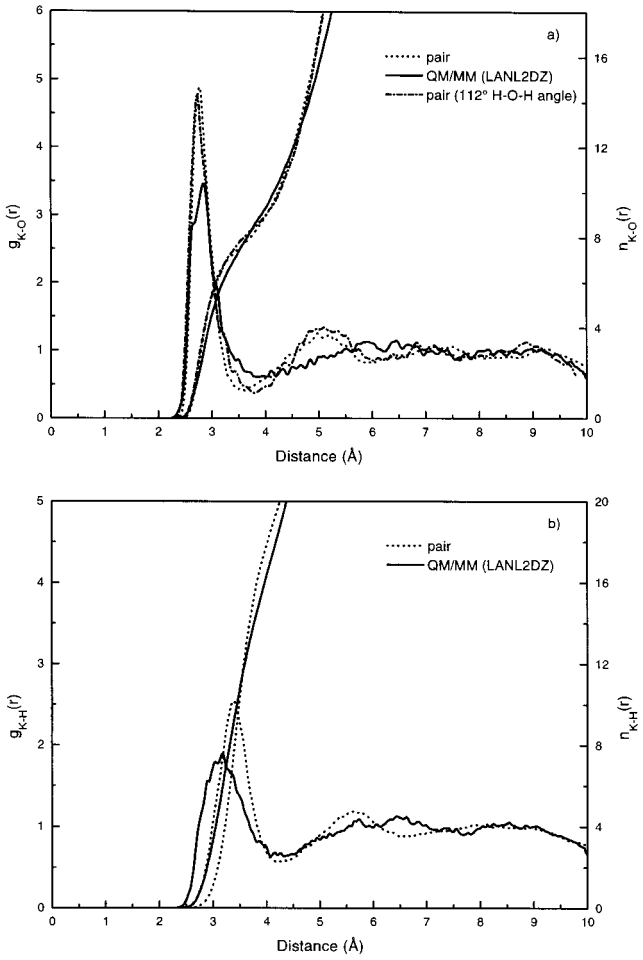

Figure 2. (a) K−O and (b) K−H radial distribution functions and their corresponding integration numbers.

respect to calculations using larger basis sets (for example, with the DZV+P basis sets for water). Only the H−O−H angle increases to ∼112°, compared to the experimental value of 104.5°. Therefore, another pair potential simulation was performed in which a fixed H−O−H angle of 112° was employed for the intramolecular potential of water. As can be seen from Figures 1a and 2a, there are no changes in the coordination numbers resulting with this larger H−O−H angle. Therefore, the observed changes in the average coordination number by the QM/MM simulations are certainly due to the effects of nonadditive contributions in the hydration shell.

3. Results and Discussion

3.1. Role of Nonadditive Terms. In Table 1, the many-body interactions are found to increase significantly with the number of ligands in the first shell. It is obvious that the pairwise additive approximation underestimates repulsion, which is reflected in the overestimation of the interaction energies. The change in the cation−oxygen distances is due to the ligand−ligand repulsion. The assumption of pairwise additivity leads to errors of 19.8% and 17.2% for the octahedral complexes of $Na(H_2O)_6^+$ and $K(H_2O)_6^+$, respectively. These values are considerably high, and it could be expected, therefore, that the nonadditive interactions can indeed play a significant role for the condensed system's structure.

3.2. Structural Data. The M−O and M−H radial distribution functions and their corresponding integration numbers obtained from classical pair potentials and combined QM/MM simulations are compared and displayed in Figures 1 and 2 for M = Na and K, respectively. For Na^+-H_2O, the Na−O peak of the pair potential simulation exhibits a first maximum at 2.36 Å, whereas the first maximum is observed at 2.33 Å in the QM/MM simulation. The first hydration shell is well separated from the second one in the pair potential simulation, leading to the coordination number of 6.5 ± 0.2. The first hydration shell of the QM/MM simulation is not clearly separated from the second one, indicating a more frequent interchange of water molecules between the first and the second shell. The average coordination number is 5.6 ± 0.3.

For K^+-H_2O, the first K−O maximum peak obtained from pair potential simulation is centered at 2.78 Å, whereas the longer distance of 2.81 Å is observed in the QM/MM simulation. The first hydration shells of both pair potential and QM/MM simulations are not clearly separated from the second ones and contain on average 7.8 ± 0.2 and 8.3 ± 0.3 water molecules, respectively.

Figure 3 shows the probability distributions of the coordination numbers, calculated up to the M−O distances of 3.2 and 3.8 Å for M = Na and K, respectively. For Na^+-H_2O, the preferred coordination number is 6 (in addition 7 and 8 are observed in decreasing amounts) in the pair potential simulation, whereas the value of 5 (and 6 in a smaller amount) is preferred according to the QM/MM simulation. In the case of the K^+-H_2O system, an inverse trend is found; a coordination number of 7 (in addition to 8 and 6 in decreasing amounts) is preferred according to the pair potential simulation, whereas 8 (followed by 9 and 7) dominates in the QM/MM simulation. To evaluate the geometrical arrangement of the water molecules around the

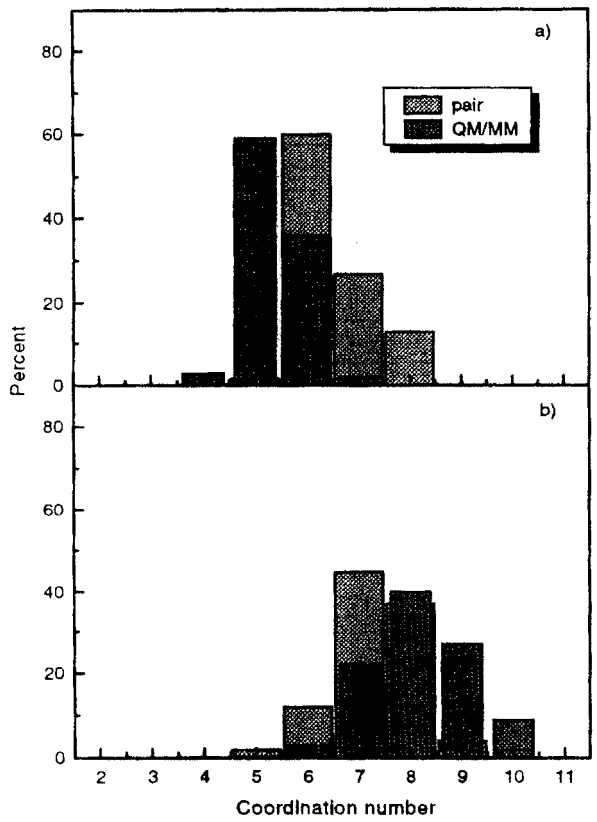

Figure 3. Coordination number distributions: (a) Na^+-H_2O; (b) K^+-H_2O.

ion, another analytical technique was applied. The ion was positioned at the origin of a Cartesian coordinate system, with the oxygen atom of the water nearest to the ion placed on the positive *z* axis, representing a reference water molecule. The other nearest-neighbor water molecules around the ion are then rotated around the *z* axis until the oxygen atom of the water molecule second nearest to the ion rests in the *xz* plane, on the positive *x* axis. Then, the positions of the oxygen atoms of all the nearest-neighbor water molecules are projected onto the *xy* plane. The density distributions of these projections are shown in Figures 4 and 5 for Na^+-H_2O and K^+-H_2O, respectively. For the hydration shell of Na^+, the distribution of water molecules clearly reveals an octahedral arrangement in both pair potential and QM/MM simulations. In the case of K^+, some structure is still recognizable from the pair potential simulation, whereas the QM/MM simulation indicates an even distribution around the ion. The hydration shell structure of Na^+ and K^+ can be further discussed on the basis of O−M−O angular distribution functions, comparing the results from pair potential and QM/MM simulations. Figure 6 displays these O−M−O angular distributions calculated up to the first minimum of the M−O RDFs. For Na^+-H_2O (Figure 6a), the pair potential simulation reveals an octahedral geometry by a well-pronounced peak around 85° and a smaller peak around 170°. In the QM/MM simulation, this octahedral structure is more distorted but still recognized from the broad peak between 85° and 110° and a small peak around 150−160°. The wider O−Na−O angle for the first peak and narrower O−Na−O angle for the small second peak are obviously related to the preferred lower coordination number in comparison with that for the pair potential simulation. The peak appearing around 60−70° and the broad shoulder from 100° to 140° can be explained by an increased flexibility in the angular orientation of water molecules in the QM/MM simulation.

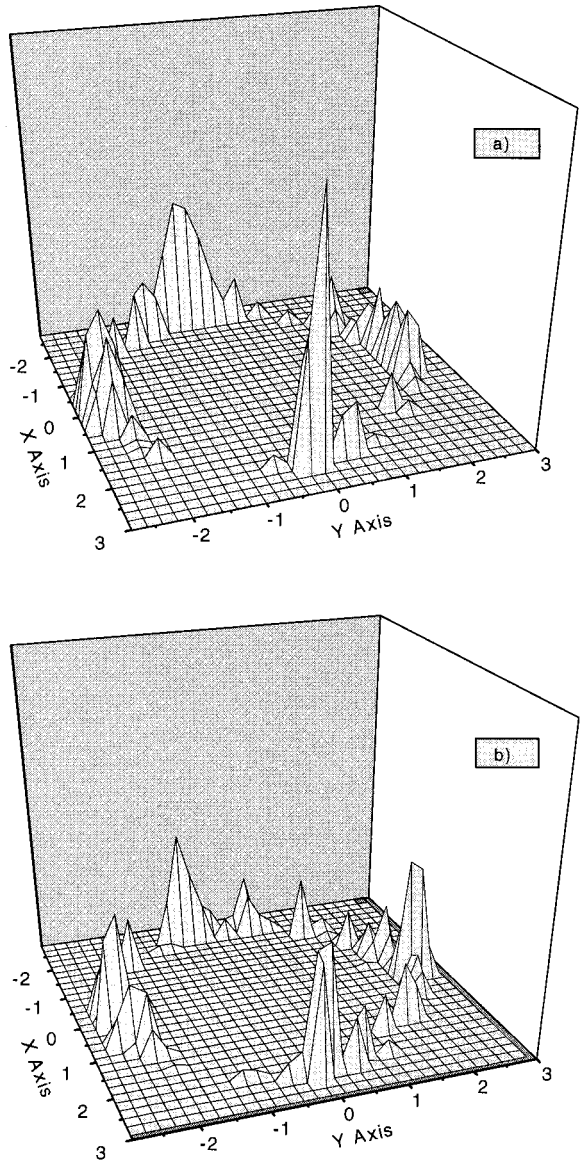

Figure 4. Three-dimensional drawing of projections of the oxygen atom positions of the nearest-neighbor water molecules around Na^+ onto the *xy* plane of the coordinate system as defined in the text, within a *z* interval of ±1 Å; (a) obtained from pair potential simulation; (b) obtained from QM/MM simulation.

For K^+-H_2O (Figure 6b), the narrower O−K−O angle indicated by the first peak in the QM/MM simulation corresponds to the accommodation of more water molecules in the first hydration shell, compared to the hydration shell resulting from the pair potential simulation. The broad peaks between 100° and 160° in both simulations prove the high flexibility of water orientation in the shell.

A comparison of hydration parameters obtained from both theoretical simulations with comparable simulation box sizes and experimental observations is given in Tables 3 and 4 for Na^+-H_2O and K^+-H_2O, respectively. In experiment, rather large discrepancies appear for the hydration numbers due to different techniques used, the different assumptions made, and the high salt concentrations, where ion pairing can have a strong influence on the structure. However, for the hydration number of Na^+, the X-ray diffraction data for the lowest concentrations (2 M and 3 M) clearly indicate coordination numbers well below 6.[12,15] For the hydration number of K^+, a rather low value of 4[10] is observed from an early total X-ray diffraction experiment,

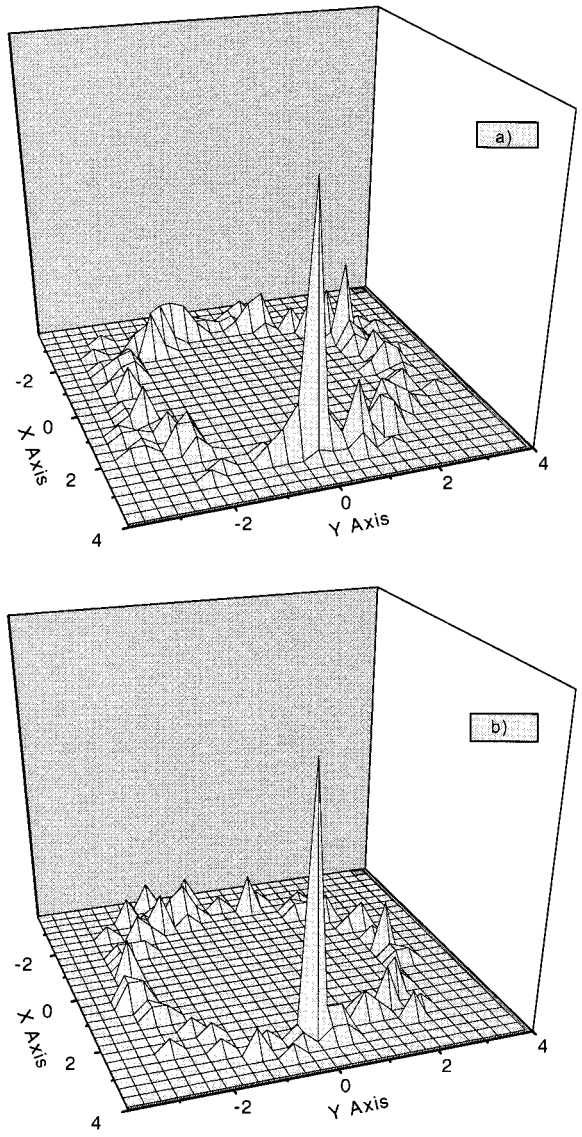

Figure 5. Three-dimensional drawing of projections of the oxygen atom positions of the nearest-neighbor water molecules around K^+ onto the *xy* plane of the coordinate system as defined in the text, within a *z* interval of ±1 Å: (a) obtained from pair potential simulation; (b) obtained from QM/MM simulation.

whereas later X-ray diffraction works yield 6.[12] The X-ray diffraction data for a weakly solvated ion like K^+ is difficult to resolve, since the K−O correlation peak is superimposed by the O−O correlation, and recourse is usually made to a model based on solid-state structures.[17] In addition, the broad peak of the K^+ total distribution function obtained from neutron diffraction also proves that K^+ is hydrated weakly enough to allow water molecules to be exchanged rapidly between the bulk and ionic hydration shells.[14]

For Na^+-H_2O, molecular dynamics simulations using three and four point transferable potential (TIP3P and TIP4P) model for water give different coordination numbers of 6.0 and 6.6, respectively.[9,7] The coordination number of 5.9 obtained from the molecular dynamics simulation using extended simple point charge (SPC/E) model for water[8] is closest to that of the QM/MM simulation in this work, but this agreement may be just incidental due to the (rather arbitrary) selection of charge parameters.

For K^+-H_2O, different coordination numbers (7.6 and 8.0) result from molecular dynamics simulations using the TIP3P

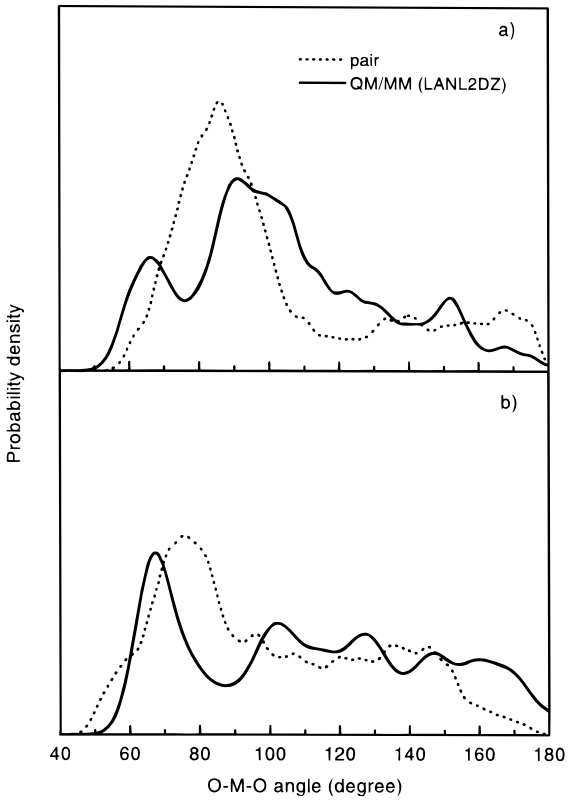

Figure 6. (a) O−Na−O and (b) O−K−O angular distributions up to the first minimum of the Na−O and K−O RDFs, respectively.

and TIP4P models for water,[9,7] as in the case of Na^+-H_2O. A lower coordination number of 7.2 is obtained from the molecular dynamics simulation using the SPC/E[8] model for water. In this case, the value of 8.3 ± 0.3 of the QM/MM simulation clearly indicates the possible failure of such effective pair potentials. The rather low coordination number of 6.3 from the Monte Carlo simulations based on the QCDF[6] model for water is probably more related to the model's inadequacy than to the failure of assumed pairwise additivity.

Another interesting feature for a comprehensive discussion of the structure of the hydrated ions and their influence on the solvent structure is the orientation of the water molecules in the first hydration sphere. The angle θ, defined by the M···O axis and the dipole vector of water has been used to characterize this orientation, once as a function of the M···O distance and once in depicting its relative distribution within the first shell. The latter shows a clear preference of the dipole-oriented arrangement in the classical pair simulations for both Na^+ and K^+ (parts a and b of Figure 7), whereas the QM/MM simulation shows a broad peak centered around 120° for Na^+, corresponding to an arrangement that albeit still stabilizing, considerably deviates from the global minimum of the pair potential function. In the case of K^+, the same arrangement is also observed, but an additional strong peak around 60° proves that a large portion of water molecules are found in configurations belonging to the destabilizing region of the pair potential function.

The observation of θ as a function of the M···O distance allows us to consider these structures within the context of further embedding of the ion in the solvent, especially with respect to a second hydration sphere. The diagrams of Figure 8 reveal a picture rather similar to that of Figure 7 concerning the first hydration shell; the pair potential overestimates the presence of dipole-oriented configurations in the immediate surrounding of both ions, whereas the QM/MM simulation

TABLE 3: Comparison of Hydration Parameters for Na^+ [a]

solute	ion/water ratio or molarity (M)	r_{max}	r_{min}	n	method	ref
Na^+	1/199	2.36	3.04	6.5 ± 0.2	CF2-water MD	this work
	1/199	2.33	2.94	5.6 ± 0.3	QM/MM MD	this work
	1/215	2.35		6.0	QCDF-water MC	6
	1/215	2.45	3.50	6.6 ± 0.1	TIP4P-water MD	7
	1/215	2.45	3.25	5.9	SPC/E-water MD	8
	1/525	2.5	3.2	6.0	TIP3P-water MD	9
NaCl	5.0 M	2.41		6	XD	11
	2.0 M	2.42		4.7	XD	12
	2.0 M	2.34		6.1	ST2-water MD	4
	0.55 M	2.30	2.95	6.1	MCY-water MC	5
	2.2 M	2.30	3.0	5.5	MCY-water MC	5
	3.35 M	2.31	3.1	5.4	MCY-water MC	5
$NaNO_3$	6.01 M	2.44		6	XD	13
	9.18M	2.44		6	XD	13
	3.13M	2.40		4.9 ± 0.1	XD	15

[a] r_{max}, r_{min}, and n are the distances of the first Na−O RDF maximum and minimum from Na^+ in Å and the coordination number of the first hydration shell, respectively).

TABLE 4: Comparison of Hydration Parameters for K^+ [a]

solute	ion/water ratio or molarity (M)	r_{max}	r_{min}	n	method	ref
K^+	1/199	2.78	3.40	7.8 ± 0.2	CF2-water MD	this work
	1/199	2.81	3.72	8.3 ± 0.3	QM/MM MD	this work
	1/215	2.71		6.3	QCDF-water MC	6
	1/215	2.70	3.65	8.0 ± 0.1	TIP4P-water MD	7
	1/215	2.80	3.65	7.2	SPC/E-water MD	8
	1/525	2.9	3.8	7.6	TIP3P-water MD	9
KOH	2.02 M	2.8		4	TXD	10
KCl	2.0 M	2.8		6	XD	12
	4.0 M	2.8		6	XD	12
	4.0 M	3.1			ND	14

[a] r_{max}, r_{min}, and n are the distances of the first K−O RDF maximum and minimum from K^+ in Å and the coordination number of the first hydration shell, respectively).

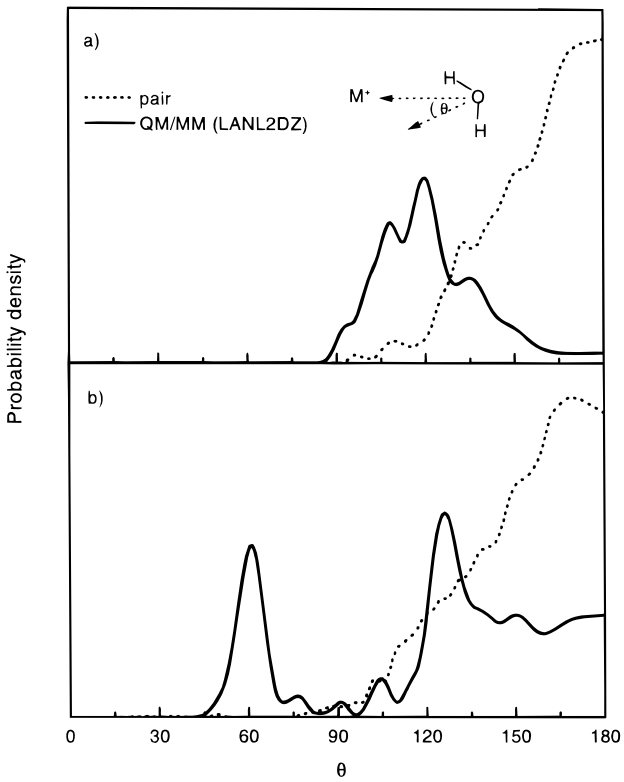

Figure 7. Distributions of θ in the first hydration shell of (a) Na^+ and (b) K^+.

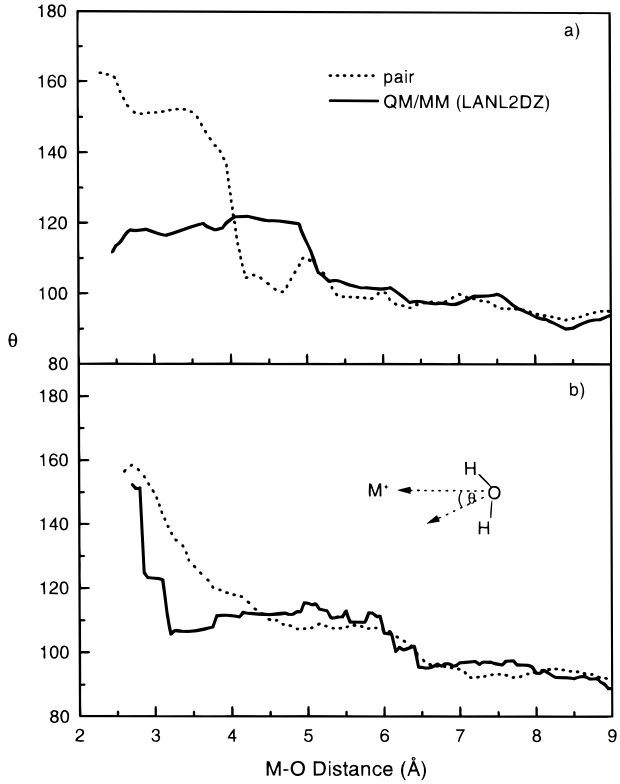

Figure 8. Average value of θ as a function of M−O distance: (a) Na^+-H_2O; (b) K^+-H_2O.

shows the configuration with $\theta = 120°$ to be dominant until a distance of 5 Å in the case of Na^+, which means there is a certain ion-induced orientation even outside the first shell. For K^+, the discrepancy between pair potential and QM/MM results is even more pronounced; θ decreases almost instantly to a value of 105°, which offers rather a better binding possibility for

TABLE 5: Some Characteristic Experimental Data Concerning Ion−Solvent Effects: *A*, Activation Energies for the Rotational Motion of Water Molecules in the Hydration Sphere of Na^+ and K^+,[56] and *B*, Orientational Potential Depth for a Water Molecule in the Hydration Sphere of Na^+ and K^+ [54]

	A (kcal·mol^{-1})		
	high-temp, 35−80 °C	low-temp, 0−25 °C	*B* (kcal·mol^{-1})
pure H_2O	3.3	4.6	≥2.3
Na^+	4.2	6.3	≥4.5
K^+	3.3	3.5	≥2.2

second-shell water molecules than for the ion. This angle is maintained up to a distance of 5.5 Å, i.e., well beyond the first hydration shell. The diagrams also prove that the transition of the QM to the MM region is smooth, without any sudden changes and/or artifacts.

These configuration data actually show that Na^+ is able to order the structure of solvent molecules in its surroundings to a considerable extent and that this effect still finds some continuation beyond the first hydration shell. Such a behavior has been postulated on the basis of experimental data and termed as "structure-making" some decades ago.[54,55] In the case of K^+, however, the unfavorable (in terms of ion−solvent interaction) arrangement of a large portion of first-shell water molecules shows that these water molecules' orientation is more strongly determined by the forces exerted by further solvent molecules in the same shell and/or the surroundings, i.e., by the attempt to form the favorable H-bond-network structure of the solvent. In this sense, the insertion of the ion can be regarded rather as a perturbation of this network structure or, as termed by solution chemists, a "structure-breaking" effect. This effect is well reflected by experimental observations,[54,55] as can be seen from the data for the activation energy for rotation of water molecules in pure water and the first hydration shells of Na^+ and K^+, respectively,[56] and from the orientational potential well depth for water molecules in pure solvent and those in these hydration spheres[54] (Table 5). These data prove a higher mobility of the water molecules in the immediate surroundings of K^+ than of those in the pure solvent, corresponding to a weakening of the solvent's H-bond network. In the case of Na^+, this mobility is reduced due to an ion−solvent binding that is stronger than the hydrogen bonding in the network.

It seems important to point out that this transition from structure-making to structure-breaking effects is not recognizable from the classical pair potential simulation, proving once more that such simulations can give only a very limited insight into the structure of hydrated ions, even in the case of weakly solvated alkali ions. The inclusion of higher interaction terms, although much more computation intensive, seems to be fully justified by this result.

Our results concerning the primary hydration shells of Na^+ and K^+ ions should gain some further importance in connection with the most recent data obtained crystallographically about the composition and structure of the potassium ion channel, which is crucial for neuron signaling and osmotic stability of cells.[57,58] In the paper of McKinnon et al.,[58] the K^+ selectivity of this channel is attributed to the rigid arrangement of carbonyl oxygens inside the channel, allowing optimal bond distances for a dehydrated K^+ ion but not for the smaller Na^+ ion. When the interaction potential surfaces of these ions with oxygen sites of ligands (water, carboxylic acids, and others investigated by ab initio methods) are considered, it must be said that a sodium ion at a less favorable distance might still reach the same or even a higher binding energy as a potassium ion at its global minimum. (In the case of H_2O, the binding energy for K^+ at the optimal distance of 2.7 Å is −18.5 kcal·mol^{-1}, whereas Na^+ still binds with −22.2 kcal·mol^{-1} at the same distance!) The crucial differences between both ions, therefore, are the energy needed to remove the first hydration shell and the orientation-related ability of the water molecules in this shell to bind preferentially to other substrates than the ion, facilitating their removal from the ion. In this context, our results about stability and structure of hydration shells provide sufficient evidence that dehydration differences between both ions should be a determining factor for the ability of the channel to uptake K^+ and not Na^+ ions.

4. Conclusion

The importance of inclusion of *n*-body terms in intermolecular potential functions even for rather weakly interacting ion−solvent systems has found another confirmation by the results of this work, and the combined QM/MM molecular dynamics approach proved once more as a very suitable and still economic way to take into account these higher terms on a quantum mechanical basis. With regard to the concrete systems investigated, the demonstration of the experimentally observed transition from structure-making to structure-breaking behavior of simple cations, depending on their interaction with the solvent and their size, as provided by this simulation technique on a molecular basis, seems to be another important feature of the results, encouraging further investigation of solute−solvent interactions by means of the QM/MM method employed in this work. Such accurate investigations seem to be of particular importance in cases where detailed energetic and structural properties of hydrated ions are needed, as could be shown here for an example of physiological relevance.

Acknowledgment. Financial support for this work from the Austrian Science Foundation (FWF), P 11683-PHY, and an Austrian government scholarship for A.T. are gratefully acknowledged.

References and Notes

(1) Birch, N. J.; Phillips, J. D. *Adv. Inorg. Chem.* **1991**, *36*, 49.
(2) Roux, B.; Karplus, M. *Annu. Rev. Biophys. Biomol. Struct.* **1994**, *23*, 731.
(3) William, R. J. P. *Bio-inorganics Chemistry*; R. F. Gould, Ed.; American Chemical Society: Washington, DC, 1971.
(4) Pálinkás, G.; Riede, W. O.; Heinzinger, K. *Z. Naturforsch.* **1977**, *32a*, 1137.
(5) Limtrakul, J. P.; Probst, M. M.; Rode, B. M. *J. Mol. Struct. (THEOCHEM)* **1985**, *22*, 23.
(6) Mezei, M.; Beveridge, D. L. *J. Chem. Phys.* **1981**, *74*, 6902.
(7) Lee, S. H.; Rasaiah, J. C. *J. Chem. Phys.* **1994**, *101*, 6964.
(8) Lee, S. H.; Rasaiah, J. C. *J. Phys. Chem.* **1996**, *100*, 1420.
(9) Obst, S.; Bradaczek, H. *J. Phys. Chem.* **1996**, *100*, 15677.
(10) Brady, G. W. *J. Chem. Phys.* **1958**, *28*, 464.
(11) Caminiti, R.; Licheri, G.; Paschina, G.; Pinna, G. *Rend. Semin. Univ. Cagliari* **1977**, *X47*, 1.
(12) Pálinkás, G.; Radnai, T.; Hajdu, F. *Z. Naturforsch.* **1980**, *35a*, 107.
(13) Caminiti, R.; Licheri, G.; Paschina, G.; Pinna, G. *J. Chem. Phys.* **1980**, *72*, 4552.
(14) Neilson, G. W.; Skipper, N. T. *Chem. Phys. Lett.* **1985**, *114*, 35.
(15) Skipper, N. T.; Neilson, G. W. *J. Phys.: Condens. Matter* **1989**, *1*, 4141.
(16) Neilson, G. W.; Enderby, J. E. *Adv. Inorg. Chem.* **1989**, *34*, 195.
(17) Neilson, G. W.; Tromp, R. H. *Annu. Rep. Phys. Chem. C* **1991**, *88*, 45.
(18) Hewish, N. A.; Neilson, G. W.; Enderby, J. E. *Nature* **1982**, *297*, 138.
(19) Howell, I.; Neilson, G. W. *J. Phys.: Condens. Matter* **1996**, *8*, 4455.

(20) Szász, G. I.; Heinzinger, K.; Pálinkás, G. *Chem. Phys. Lett*. **1981**, *78*, 194.
(21) Spohr, E.; Pálinkás, G.; Heinzinger, K.; Bopp, P.; Probst, M. M. *J. Phys. Chem*. **1988**, *92*, 6754.
(22) Bopp, P.; Heinzinger, K.; Jancsò, G. *Z. Naturforsch*. **1977**, *32a*, 620.
(23) Heinzinger, K. *Pure Appl. Chem*. **1991**, *63*, 1733.
(24) Guàrdia, E.; Padró, J. A. *Chem. Phys*. **1990**, *144*, 353.
(25) Yamaguchi, T.; Ohtaki, H.; Spohr, E.; Pálinkás, G.; Heinzinger, K.; Probst, M. M. *Z. Naturforsch*. **1986**, *41a*, 1175.
(26) Kistenmacher, H.; Popkie, H.; Clementi, E. *J. Chem. Phys*. **1974**, *61*, 799.
(27) Clementi, E.; Kistenmacher, H.; Kolos, W.; Romano, S. *Theor. Chim. Acta*. **1980**, *55*, 257.
(28) Curtiss, L. A.; Halley, J. W.; Hautman, J. *Chem. Phys*. **1989**, *133*, 89.
(29) Probst, M. M. *Chem. Phys. Lett*. **1987**, *137*, 229.
(30) Kollman, P. A.; Kuntz, I. D. *J. Am. Chem. Soc*. **1974**, *96*, 4766.
(31) Lybrand, T. P.; Kollman, P. A. *J. Chem. Phys*. **1985**, *83*, 2923.
(32) Ortega-Blake, I.; Novaro, O.; Lès, A.; Rybak, S. *J. Chem. Phys*. **1982**, *76*, 5405.
(33) Gonzàlez-Lafont, A.; Lluch, J. M.; Oliva, A.; Bertràn, J. *Int. J. Quantum Chem*. **1986**, *30*, 663.
(34) Bounds, D. G. *Mol. Phys*. **1985**, *54*, 1335.
(35) Kerdcharoen, T.; Liedl, K. R.; Rode, B. M. *Chem. Phys*. **1996**, *211*, 313.
(36) Tongraar, A.; Liedl, K. R.; Rode, B. M. *J. Phys. Chem. A* **1997**, *101*, 6299.
(37) Tongraar, A.; Liedl, K. R.; Rode, B. M. *Chem. Phys. Lett*. **1998**, *286*, 56.
(38) Yongyai, Y. P.; Kokpol, S.; Rode, B. M. *Chem. Phys*. **1991**, *156*, 403.
(39) Hannongbua, S.; Kerdcharoen, T.; Rode, B. M. *J. Chem. Phys*. **1992**, *96*, 6945.
(40) Marini, G. W.; Texler, N. R.; Rode, B. M. *J. Phys. Chem*. **1996**, *100*, 6808.
(41) Warshel, A.; Levitt, M. *J. Mol. Biol*. **1976**, *103*, 227.
(42) Field, M. J.; Bash, P. A.; Karplus, M. *J. Comput. Chem*. **1990**, *11*, 700.
(43) Gao, J. *J. Phys. Chem*. **1992**, *96*, 537.
(44) Hannongbua, S. *Chem. Phys. Lett*. **1998**, *288*, 663.
(45) Dunning, T. H. Jr.; Hay, P. J. *Modern Theoretical Chemistry*; Schaefer, H. F., III, Ed.; Plenum: New York, 1976; p 1.
(46) Hay, P. J.; Wadt, W. R. *J. Chem. Phys*. **1985**, *82*, 270.
(47) Dzidic, I.; Kerbarle, P. *J. Phys. Chem*. **1970**, *74*, 1466.
(48) Stillinger, F. H.; Rahman, A. *J. Chem. Phys*. **1978**, *68*, 666.
(49) Bopp, P.; Jancsó, G.; Heinzinger, K. *Chem. Phys. Lett*. **1983**, *98*, 129.
(50) Frisch, M. J.; Trucks, G. W.; Schlegel, H. B.; Gill, P. M. W.; Johnson, B. G.; Robb, M. A.; Cheeseman, J. R.; Keith, T. A.; Peterson, G. A.; Montgomery, J. A.; Raghavachari, K.; Al-Laham, M. A.; Zakrzewski, V. G.; Ortiz, J. V.; Foresman, J. B.; Cioslowski, J.; Stafanov, B. B.; Nanayakkara, A.; Challacombe, M.; Peng, C. Y.; Ayala, P. Y.; Chen, W.; Wong, M. W.; Andres, J. L.; Replogle, E. S.; Gomperts, R.; Martin, R. L.; Fox, D. J.; Binkley, J. S.; Defrees, D. J.; Baker, J.; Stewart, J. P.; Head-Gordon, M.; Gonzalez, C.; Pople, J. A. *GAUSSIAN 94*; Gaussian, Inc.: Pittsburgh, PA, 1995.
(51) Kistenmacher, H.; Popkie, H.; Clementi, E. *J. Chem. Phys*. **1973**, *59*, 5842.
(52) Adams, D. J.; Adams, E. H.; Hills, G. J. *Mol. Phys*. **1979**, *38*, 387.
(53) Brooks, B. R.; Bruccoleri, R. E.; Olafson, B. D.; States, D. J.; Swaminathan, S.; Karplus, M. *J. Comput. Chem*. **1983**, *4*, 187.
(54) Hertz, H. G. *Water, A Comprehensive Treatise*; Plenum Press: New York, 1973; Vol. 3, Chapter 7.
(55) Bockris, J. O'M.; Reddy, A. K. N. *Modern Electrochemistry*; Plenum Press: New York, 1970; Vol. 1, p 72.
(56) Endom, L.; Hertz, H. G.; Thül, B.; Zeidler, M. D. *Ber. Bunsen-Ges. Phys. Chem*. **1967**, *71*, 1008.
(57) Armstrong, C. *Science* **1998**, *280*, 56.
(58) Doyle, D. A.; Cabral, J. M.; Pfuetzner, R. A.; Kuo, A.; Gulbis, J. M.; Cohen, S. L.; Chait, B. T.; MacKinnon, R. *Science* **1998**, *280*, 69.